Heliyon 5 (2019) e02375

Contents lists available at ScienceDirect

Heliyon

journal homepage: www.heliyon.com

Distribution and Co-localization of endosome markers in cells

Lindsay J. Shearer [a,b,*], Nils O. Petersen [a,b]

[a] Department of Chemistry, University of Alberta, Edmonton, AB, T6G 2G2, Canada
[b] National Institute for Nanotechnology, National Research Council, Edmonton, AB, T6G 2M9, Canada

ARTICLE INFO

Keywords:
Analytical chemistry
Physical chemistry
Biophysics
Cell biology
Cell imaging
Image correlation spectroscopy
Endocytosis
Fluorescence microscopy

ABSTRACT

Clathrin mediated endocytosis is one pathway for internalization of extracellular nano materials into cells [1, 2]. In this pathway, proteins attached to receptors and the internalized materials are encapsulated in clathrin coated membrane vesicles that subsequently fuse with or transform into intracellular compartments (early and late endosomes) as their contents are being directed to the lysosomes for degradation. The following proteins are commonly used to mark the pathway at various stages: Rab5 (early endosome), Rab7 (late endosome), and LAMP-1 (lysosome). In this work, we studied the distribution and co-localization of these marker proteins in two cell lines (C2C12 and A549) to determine whether these markers are unique for specific endosome types or whether they can co-exist with other markers. We estimate the densities and sizes of the endosomes containing the three markers, as well as the number of marker antibodies attached to each endosome. We determine that the markers are not unique to one endosome type but that the extent of co-localization is different for the two cell types. In fact, we find endosomes that contain all three markers simultaneously. Our results suggest that the use of these proteins as specific markers for specific endosome types should be reevaluated. This was the first successful use of triple image cross correlation spectroscopy to qualitatively and quantitatively study the extent of interaction among three different species in cells and also the first experimental study of three-way interactions of clathrin mediated endocytic markers.

1. Introduction

Clathrin mediated endocytosis is one process known to take up extracellular, nanosized, materials through membrane invaginations that rely on the recruitment of clathrin from the cytoplasm to the membrane [1, 2, 3, 4, 5, 6]. This endocytic pathway then involves the formation of intracellular vesicles that transform into various endocytic compartments [7]. There are a series of maturation and fusion steps that are hypothesized to occur as the endosomes transform from early to late endosomes and then to lysosomes [8]. Two models have been proposed; the vesicle shuttle model and the maturation model [9, 10]. The vesicle shuttle *model* proposes that the endosomes are of fixed size, location, and morphology and transport of cargo occurs by smaller vesicles transporting the cargo between the endosomes. In this model specific endosomal markers could be uniquely associated with a particular endosome compartment. The maturation model proposes that the endosomes and their contents remain together as the endosomes undergo maturation and subsequent fusion with the lysosome. In this model, intracellular protein markers for the various endosomes could co-exist during the maturation and fusion process. The latter model appears to be the most commonly supported by evidence to date [11, 12, 13, 14, 15], but more specific, direct evidence for the simultaneous presence of two or more markers on the same endosomes is missing.

The Rab-GTPase (Rab) family of proteins are associated with intracellular membrane trafficking and Rab proteins have been identified to localize to specific domains on endocytic compartments [16, 17]. These specific Rab proteins are therefore referred to as *markers* for early and late endosomes. In particular, Rab5 is used as a marker for early endosomes [18, 19, 20, 21, 22, 23] and Rab7 is used as a marker for late endosomes [24, 25, 26, 27, 28]. No Rab proteins have been identified to localize specifically to the lysosome, however the lysosomal associated membrane protein (LAMP-1) is known as a marker for the lysosomes [29, 30, 31, 32, 33]. In this work, we used antibodies against Rab5, Rab7, and LAMP-1 to study their distribution and possible co-localization within the cell.

Fluorescence microscopy has been used to *visualize* the co-localization of cargo with intracellular proteins and membranes [14, 34, 35]. In addition, it has also been used to determine the distribution of various endocytic organelles based on association of Rab proteins with intracellular membranes [36], the dynamics of clathrin recruitment to the cell

* Corresponding author.
E-mail address: lindsay@ualberta.ca (L.J. Shearer).

https://doi.org/10.1016/j.heliyon.2019.e02375
Received 13 June 2019; Received in revised form 19 August 2019; Accepted 22 August 2019

membrane [37, 38], the dynamics of adapter protein recruitment and removal [39], and the dynamics of dynamin assisted pinching of the invaginated pit [40, 41]. However, no quantitative studies have been performed to determine the extent of co-localization and clustering of Rab5, Rab7, and LAMP-1 markers in cells.

The purpose of this work was to determine as quantitatively as possible, the density of markers on the endosomes, the size of the endosomes, whether markers for the early endosome (Rab5), the late endosome (Rab7) and the lysosome (LAMP-1) can coexist on the endosomes and whether these observations depend on the type of cell being studied.

2. Methods

Cell culture and sample labelling experiments were done at the National Institute for Nanotechnology (NINT) in Edmonton, Alberta. Fluorescent imaging was done at the Cell Imaging Facility at the Cross Cancer Institute in Edmonton, Alberta.

2.1. Cell culture

Mouse muscle myoblastoma (C2C12) cells were cultured in Dulbecco's modified eagle medium (DMEM), supplemented with 10 % fetal bovine serum (FBS). Human alveolar adenocarcinoma (A549) cells were cultured in Ham's F-12 K medium (F-12 K) supplemented with 10 % FBS. The cells were grown in an incubator chamber maintained at 37 °C and with 5 % Carbon Dioxide (CO_2) atmosphere and were passaged every five days using 0.25 % Trypsin-EDTA. At 80% cell surface confluence, the cells were passaged 1:5 onto 35 mm (mm) glass bottom dishes and maintained in a 37 °C, 5 % CO_2 incubator for about two days when approximately 60 % cell confluency was reached for experimentation. At this time the media was replaced with 1 mL of fresh media and treated as indicated below.

2.2. Immunofluorescent labelling

Labeling of the various endocytic compartments was accomplished with antibodies specific for Rab5, Rab7, and LAMP-1 protein endocytic markers. The primary antibodies used were monoclonal and originated from three different species (mouse, rabbit, and rat) to avoid potential crosslinking in experiments with multiple labels. Polyclonal secondary antibodies labeled with different fluorescent probes were added to bind with the primary antibodies. The fluorescent probes of the polyclonal antibodies were labelled and identified by the manufacturer as Cy3, Alexa Fluor 488 nm, Alexa Fluor 555 nm, and Alexa Fluor 647 nm.

2.2.1. Labeling one endocytic marker

At 60% cell surface confluency, the cells were exposed to 1 mL of 4 % paraformaldehyde (PFA) at room temperature for 15 min for cell fixation. They were then washed with 1X phosphate buffered saline (PBS) and permeabilized with 1 mL of a 0.3% solution of Triton X-100 detergent in 1X PBS for 15 min at 37 °C. The cells were washed with 1X PBS, and exposed to 100 μL of a 3 % solution of Bovine Serum Albumin (BSA) in 1X PBS to minimize non-specific intracellular binding of the antibodies.

Next, the cells were washed with 1X PBS and labelled with the primary antibody of interest using 100 μL of the diluted (1:100) primary antibody solution overnight at 4 degrees Celsius. Finally, cells were washed with 1X PBS and labelled with the diluted (1:400 for Alexa Fluor 647 nm, 1:500 for Cy3, Alexa Fluor 488 nm, and Alexa Fluor 555 nm) secondary antibody for 90 min at room temperature and then washed with 1X PBS for the last time before imaging.

2.2.2. Labeling two endocytic markers

To study the extent of colocalization of two markers, the following three combinations were studied: Rab5 and Rab7 markers; Rab5 and LAMP-1 markers; and Rab7 and LAMP-1 markers.

Pairs of primary and secondary antibodies were carefully selected to avoid potential for cross-reactions. Specifically, we used the following combinations in this sequence; 1) Mouse-Anti Rab5 and Goat Anti-Mouse Cy3 with Rabbit Anti-Rab7 and Goat Anti-Rabbit Alexa Fluor 647, 2) Mouse-Anti Rab5 and Goat Anti-Mouse Cy3 with Rat Anti-LAMP-1 and Goat Anti-Rat Alexa Fluor 647, 3) Rabbit Anti-Rab7 and Goat Anti-Rabbit Alexa Fluor 647 with Rat Anti-LAMP-1 and Goat Anti-Rat Alexa Fluor 555.

Once samples were labelled with one primary and secondary antibody pair as described for one endocytic marker, the cells were washed with 1X PBS at room temperature, and then exposed to the second primary and secondary antibody pair of interest using the same procedure.

2.2.3. Labeling three endocytic markers

To determine the extent of co-localization of all three markers, the cells were labeled with primary and secondary antibody pairs for Rab5, then Rab7, and finally Lamp-1 using Mouse-Anti Rab5 and Goat Anti-Mouse Cy3; Rabbit Anti-Rab7 and Goat Anti-Rabbit Alexa Fluor 647; and Rat Anti-LAMP-1 and Goat Anti-Rat Alexa Fluor 488.

2.3. Image acquisition

Images of the cells in a sample were obtained with a Carl Zeiss 710 Laser Scanning Confocal Microscope with a 63 × 1.4 Numerical Aperture Oil DIC Plan-Apochromatic lens. ZEN 2011 was the software used to adjust and select parameters for image acquisition.

Lasers used for image acquisition were Argon Ion for Fluorescein Isothiocyanite (FITC) configuration (488 nm excitation of the Alexa Fluor 488 nm probe), Solid State for Cyanine-3 (Cy3) Configuration (561 nm excitation of the Cy3 and Alexa Fluor 555 nm probes), and HeNe for Cyanine-5 (Cy5) Configuration (633 nm excitation of the Alexa Fluor 647 nm probe). Complementary DIC was used for focusing.

The detectors for each configuration were adjusted in such a way that the emission from each channel was unique to a specific wavelength range. In addition, as a control measure, samples labelled with one fluorescent probe, such as Cy3, were illuminated with the FITC configuration, and then with the Cy5 configuration separately, to establish that potential cross talk was minimized (see supplemental). In addition, controls showed that there was little non-specific binding of secondary antibodies (see supplemental).

The pixel dwell time was set to 3.15 μs (μs) with an average of 2 line scans, and the pinhole was set to 1 airy-unit (AU). A Zoom factor of 14 was used to achieve a pixel size of approximately 20 nm. Each image comprised a square of 512 × 512 pixels, resulting in a 10 × 10 micron image for image correlation spectroscopy analysis. For each experiment, 25–40 images were obtained; each image recorded from a different cell in the sample.

2.4. Image J & ICS software for ICS family analysis

In this study, the image correlation toolkit in ImageJ software was utilized and the following pieces of information from images were obtained: the normalized auto and cross correlation function amplitudes, the average image intensity, and the laser beam radius in microns. Regions of interest were selected to 256 × 256 of the 512 × 512 image to avoid dark regions of the image where there is no cell. Cross correlation of images from two channels from two *different* cells to determine the cross-correlation amplitude that can arise from uncorrelated fluctuations. This represents a lower limit for the significance of cross correlation amplitude arising from two channels from the *same* cell.

For TRICCS measurements, images were analyzed using image correlation spectroscopy software written by Dr. Max Anikovsky (manuscript in preparation). Parameters for the range of data points, triple cross correlation amplitude, laser beam radius, and correlation value at infinite limits were estimated to obtain the auto, cross, and triple correlation functions amplitudes, and intensities for single, double, and triple color

images, in various combinations.

3. Materials

C2C12 and A549 cells were obtained from American Type Culture Collection™. Dulbecco's modified eagle medium (DMEM), fetal bovine serum (FBS), and 0.25% Trypsin-EDTA were obtained from Invitrogen Life Technologies™.

PFA was obtained from EMD®.

Primary antibodies specific for Rab5 and LAMP-1 were obtained from Abcam®. Primary antibodies specific for Rab7 were obtained from Cell Signaling Technology®. All primary antibodies used were monoclonal. Secondary antibodies for Rab7, and LAMP-1 were obtained from Cell Signaling Technology®. Secondary antibody specific for Rab5 was obtained from Abcam®.

4. Theory

Image correlation spectroscopy (ICS) is a quantitative method used to analyze the fluorescent intensity fluctuations in an image obtained from a laser scanning confocal microscope. This analysis allows one to retrieve: the average intensity of markers, the number of marked endosomes, the number of marked endosomes per square micron, the relative degree of aggregation of markers per endosome, and the extent of co-localization between two or three markers of interest on an endosome.

4.1. Image correlation spectroscopy (ICS) theory

Image Correlation Spectroscopy (ICS) is an intensity fluctuation analysis of images obtained using a laser scanning confocal microscope in which relative fluctuations in intensity, $\delta_n i(x,y)$, are used to calculate a normalized auto correlation function, $g(\alpha,\beta)$ where α and β are lag distances in the images [42].

In the limit as α and β approach zero, the amplitude of the normalized auto correlation function, denoted by $g(0,0)$, becomes the variance of the intensity fluctuations [43];

$$g(0,0) = var(\delta_n i(x,y)) \tag{1}$$

Whenever the intensity is proportional to the concentration of fluorescent probes (here fluorescent markers), the variance can be shown to be the inverse of the average number of fluorescent markers or clusters of fluorescent markers – here the marked endosomes, N_E - in the observation region;

$$g(0,0) = var(\delta_n i(x,y)) = \frac{1}{\langle N_E \rangle} \tag{2}$$

The cross-sectional area of the observation volume is given by $\pi\omega^2$, where ω is the e^{-2} beam radius. Thus, we define the average number of marked endosomes per square micron, the Endosome Density (ED), as:

$$ED = \frac{1}{g(0,0)\pi\omega^2} = \frac{\langle N_E \rangle}{\pi\omega^2} \tag{3}$$

The average intensity is proportional to the number of fluorescent markers, $\langle i(x,y) \rangle = c\langle N_M \rangle$, where c is a proportionality constant reflecting spectroscopic and optical parameters such as emission collection efficiency, quantum yields, and molar adsorption coefficients [42]. We define the degree of aggregation *DA*, as:

$$DA = \langle i(x,y) \rangle g(0,0) = c\frac{\langle N_M \rangle}{\langle N_E \rangle} \tag{4}$$

This is an estimate of the average number of fluorescent markers per endosome.

4.1.1. Image cross correlation spectroscopy (ICCS) theory

Image cross correlation spectroscopy (ICCS) is an extension of ICS that enables the analysis of images collected from two markers labelled with two different colors, say green (g) and red (r) [44].

Using ICCS we calculate the auto correlation amplitudes, $g_g(0,0)$ and $g_r(0,0)$, and the cross-correlation amplitude $g_{gr}(0,0)$. The average number of endosomes that contain both green and red markers, N_{gr}, can be estimated from the cross correlation and individual auto correlation amplitudes:

$$\langle N_{gr} \rangle = \frac{g_{gr}(0,0)}{g_g(0,0)g_r(0,0)} \tag{5}$$

The extent of co-localization can be represented as fractions of endosomes with one marker that also contain the other:

$$F(g|r) = \frac{\langle N_{gr} \rangle}{\langle N_g \rangle} = \frac{g_{gr}(0,0)}{g_r(0,0)} \tag{6}$$

$$F(r|g) = \frac{\langle N_{gr} \rangle}{\langle N_r \rangle} = \frac{g_{gr}(0,0)}{g_g(0,0)} \tag{7}$$

Eq. (6) defines the fraction of endosomes containing green markers that also have red markers. Correspondingly, Eq. (7) defines the fraction of endosomes containing red markers that also have green markers.

4.1.2. Triple image cross correlation spectroscopy (TRICCS)

Triple Image Cross Correlation Spectroscopy (TRICCS) is a further extension of ICCS that enables the analysis of images of three colored markers to estimate the extent of co-localization of all three species, green (g), red (r), and blue (b).

The average number of endosomes that contain green, red, and blue markers, N_{grb}, can be estimated from the triple cross correlation amplitude and the individual auto correlation amplitudes [36]:

$$\langle N_{grb} \rangle = \frac{g_{grb}(0,0,0,0)}{g_g(0,0)g_r(0,0)g_b(0,0)} \tag{8}$$

The fraction of endosomes containing one marker that contain both of the other markers are:

$$F(g|rb) = \frac{\langle N_{grb} \rangle}{\langle N_g \rangle} = \frac{g_{grb}(0,0,0,0)}{g_r(0,0)g_b(0,0)} \tag{9}$$

$$F(r|gb) = \frac{\langle N_{grb} \rangle}{\langle N_r \rangle} = \frac{g_{grb}(0,0,0,0)}{g_g(0,0)g_b(0,0)} \tag{10}$$

$$F(b|rg) = \frac{\langle N_{grb} \rangle}{\langle N_b \rangle} = \frac{g_{grb}(0,0,0,0)}{g_r(0,0)g_g(0,0)} \tag{11}$$

As an example, Eq. (9) defines the fraction of endosomes that contain green markers that also contain both red and blue markers.

5. Results

5.1. Distribution of markers and endosome size is cell type specific

We examined endosome markers on singly labeled cells to understand their distribution using imaging and ICS analysis. We observed the average intensity and the amplitude of the correlation functions were both orders of magnitude greater than for the control samples for which either the primary or the secondary antibody was omitted in the labelling steps. Thus, the measurement of the intensity of markers in the observation area is specific and well above background intensity.

Fig. 1 shows contrast enhanced fluorescence microscopy images of three different C2C12 cells. Each cell was labelled individually with antibodies for Rab5, Rab7, or LAMP-1. Approximately 40 images (from 40 different cells) were obtained for each of the three single label

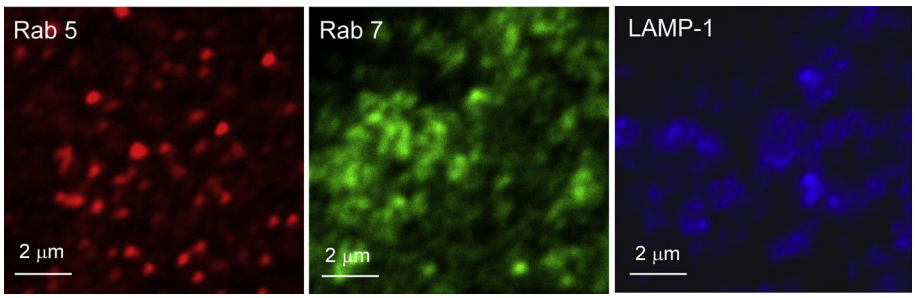

Fig. 1. Rab5, Rab7, and LAMP-1 Marked Endosomes in C2C12 cells.

experiments.

The images Fig. 1 show that the bright regions of Rab7 and LAMP-1 appear larger than those of Rab5. It is important to note that the quality of the images is determined by the resolution of the microscope and by the contrast of the objects. These objects are small and do not appear to have sharp edges. Therefore, they may appear blurry but that is the nature of the objects. In addition, these images are obtained at a high resolution so most of the objects are on the micron scale. Finally, the images are oversampled so that they can be used for image correlation analysis which makes them appear blurry.

Fig. 2 shows contrast enhanced fluorescence microscopy images of three different A549 cells. Each cell was labelled individually with antibodies for Rab5, Rab7, and LAMP-1. Approximately 30 images were obtained for each of the three single label experiments.

The images shown in Fig. 2 show that each marked endosome appears to be similarly distributed over the entire image.

Table 1 shows the averages of the fitted laser beam width, ω (μm), and average number of clusters (endosomes), N_E, per unit area for C2C12 and A549 cells. These parameters were obtained by ICS analysis and averaged over the number of images indicated for each.

The average number of endosomes per unit area ranges from 2-6, consistent with a highly clustered pattern of fluorescence. There does not appear to be a consistent pattern of densities between the different markers or the two cell types.

The average width of the correlation function is slightly larger for the Rab7 and LAMP-1 in C2C12 cells but is smaller and more variable in A549 cells. Theoretically, we expect the laser beam width to range from 0.17 to 0.22 μm for the 488, 561, and 633 nm lasers with the optics used in these experiments. In all cases, the beam widths presented in Table 1, which refer to the widths of the correlation functions, are larger than the expected beam widths. This suggests that there may be a convolution effect between finite sized endosomes and the laser beam. We can model this convolution (see supplemental) and use it to estimate the actual endosome sizes as shown in Table 2.

These values compare well with other work, in which the endocytic vesicles have been determined to range in size from 0.2-0.6 μm using confocal and electron microscopy [45, 46].

Because the intensity of fluorescence emitted from a sample labelled with only secondary antibodies should correspond to non-specific binding of individual secondary antibodies, we measured the number of individual antibodies per cluster (see supplemental) using the intensities and amplitudes of the autocorrelation functions corresponding to samples labeled with only secondary antibodies [47, 48]. We estimated that

Table 2
Measured beam width and object radius in C2C12 and A549 Cells.

Marker	C2C12		A549	
	$\langle \omega\ (\mu m) \rangle$	$\langle r\ (\mu m) \rangle$	$\langle \omega\ (\mu m) \rangle$	$\langle r\ (\mu m) \rangle$
Rab-5	0.32	0.34	0.31	0.31
Rab-7	0.48	0.62	0.43	0.52
LAMP-1	0.49	0.64	0.33	0.42

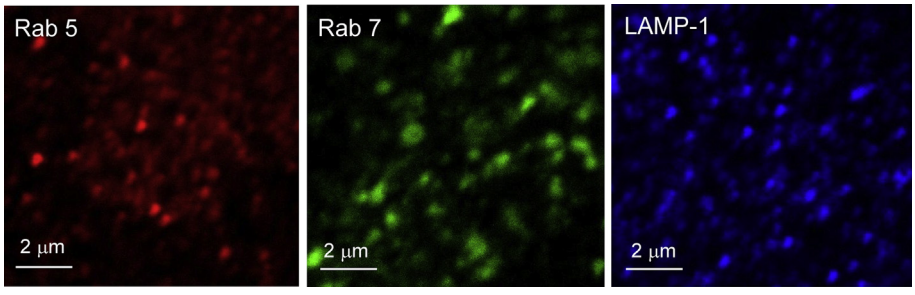

Fig. 2. Rab5, Rab7, and LAMP-1 Marked Endosomes in A549 cells.

Table 1
Summary of averaged ICS parameters for cells labelled for marked endosomes in C2C12 and A549 cells.

Marker	C2C12			A549		
	n_{images}	$\langle \omega\ (\mu m) \rangle$	$\langle N_E \rangle$	n_{images}	$\langle \omega\ (\mu m) \rangle$	$\langle N_E \rangle$
Rab-5	38	0.32 ± 0.01[1]	5.7 ± 0.4	31	0.31 ± 0.01	4.8 ± 0.6
Rab-7	37	0.48 ± 0.06	4.2 ± 0.4	26	0.43 ± 0.06	1.9 ± 0.2
LAMP-1-488	35	0.47 ± 0.01	2.2 ± 0.1	30	0.28 ± 0.01	4.9 ± 0.4
LAMP-1-561	41	0.50 ± 0.01	2.9 ± 0.2	32	0.36 ± 0.01	2.2 ± 0.2
LAMP-1-633	41	0.51 ± 0.01	2.6 ± 0.1	26	0.33 ± 0.01	11 ± 1

[1] Standard error.

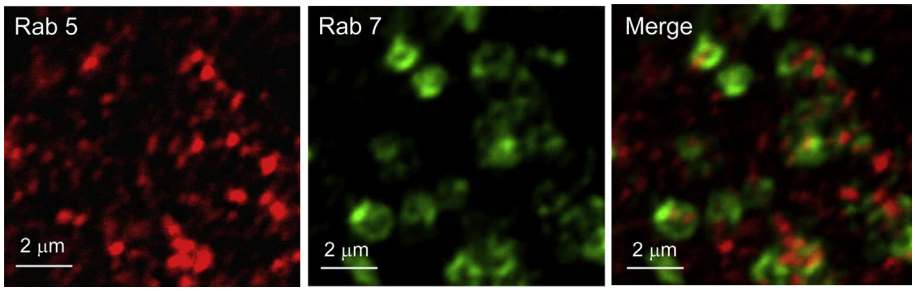

Fig. 3. Rab5-561 & Rab7-633 marked endosomes in C2C12 cells.

there are approximately 1000 Rab5 and Rab7 antibodies per endosome in C2C12 cells and approximately 500 Rab5 and Rab7 antibodies per endosome in A549 cells. We did not get reliable estimates for the number of LAMP-1 antibodies because the non-specific binding of that secondary antibody was too low.

5.2. Endosomal markers are not unique to one compartment

Fig. 3 shows contrast enhanced images of antibodies to Rab5 (Rab5-561, in red) and antibodies to Rab7 (Rab7-633, in green) in the same cell. The Merge image is an overlay of the Rab5-561 and Rab7-633 contrast enhanced images.

In Fig. 3, several yellow and orange regions are observed in the Merge image, implying that there is some degree of co-localization of Rab5-561 and Rab7-633 markers.

Table 3 shows the average number of clusters containing Rab5, Rab7, and both, as well as the fractions as defined by Eqs. (6) and (7) obtained by ICCS analysis from measurements on 30–40 cells.

The average number of endosomes containing Rab5 or Rab7 are observed to be just over twice the number of endosomes that contain both Rab5 and Rab7 markers, suggesting that there are a significant number of endosomes that contain both markers. The average fractions of co-localization represented in Table 3 are calculated as an average of 30–40 individual fractions (as compared to a fraction of the averages) and reflect that on average approximately 46% of the endosomes that contain Rab5-561 markers also contain Rab7-633 markers and approximately 53% of the endosomes containing Rab7-633 markers also contain Rab5-561 markers. The observation that about half of the endosomes contain both markers show that these markers are not unique to a specific endosome type since they can coexist on the same endosomes. While this was suggested by the images, the more quantitative ICCS approaches gives better insight into the extent of co-existence.

Fig. 4 shows examples of three merged images of C2C12 cells doubly labelled for Rab5-561 and Rab7-633; Rab5-561 and LAMP-1-633; and Rab7-633 and LAMP-1-561 markers.

The images in Fig. 4 show various degrees of yellow and orange indicating some degree of co-localization of all pairs of markers. For example, there are a significant number of yellow regions in the image corresponding to Rab7 and LAMP-1.

Table 4 summarizes the calculated average values of fractions of co-localization for each pairwise interaction studied in C2C12 cells (including the data from Table 3).

Table 3
Average number of endosomes containing markers and fractions of Co-Localization of Rab5 & Rab7 markers in C2C12 cells.

Marker	$\langle N_E \rangle$	$\langle F(Rab5\|Rab7) \rangle$	$\langle F(Rab7\|Rab5) \rangle$
Rab5-561	5.4 ± 0.5[1]		
Rab7-633	5.5 ± 0.9		
Rab5-561 & Rab7-633	2.2 ± 0.3	0.46 ± 0.05	0.53 ± 0.06

[1] Standard error.

The results presented in Table 4 show that there is some co-localization of all the endosome and lysosome markers, but to different extents. Of those endosomes containing Rab5, 46% also contain Rab7, and 32% also contain LAMP-1. Of those endosomes containing Rab7, 53% also contain Rab5 and 74% also contain LAMP-1. Of those lysosomes that contain LAMP-1, 31% also contain Rab5 and 86% also contain Rab7.

The observation that Rab5 and Rab7 markers co-localize is consistent with the early endosomes maturing into the late endosomes; it may take some time before the Rab5 is cleared from the endosomes. Those endosomes that contain Rab5 but not Rab7 may then be early endosomes prior to maturation while those that contain Rab7 but not Rab5 may be even later stage endosomes from which the Rab5 has been cleared.

The observation that Rab7 and LAMP-1 markers co-localize to between 74% and 86% is consistent with the process of fusion of the late endosome into a lysosome and that the process to clear all the Rab7 from the lysosome is very slow.

The observation that Rab5 and LAMP-1 markers co-localize to a significant extent is surprising and suggests that the Rab5 is not cleared completely from the late endosome before it fuses with the lysosome. This observation coupled with the nearly complete co-localization of Rab7 and LAMP-1, further suggests that there must be endosomes which contain all three markers simultaneously. To test this, we performed triple labeling experiments and analyzed these using triple cross-correlation spectroscopy (*vide infra*).

Table 5 summarizes the calculated averaged fractions of co-localization for each pairwise interaction in A549 cells.

Table 5 shows once again that there is a significant co-localization of all the endosome and lysosome markers, but the extent of co-localization is different in the A549 cells when compared to C2C12 cells. In the A549 cells, the co-localization between Rab5 and LAMP-1 is much higher (about 80%) and the co-localization between Rab7 and LAMP-1 is much smaller (about 25–35%). This suggests that in these cells some of the early endosomes that contain only Rab5 may fuse directly with the lysosomes prior to the maturation process that form the late endosomes. This is different from the observations for C2C12 cells which may reflect the difference in the way these cell types process internalized materials. We note that the A549 cell is derived from pulmonary type II cells which have the function of recycling lipids from the pulmonary air-water interface and forming lamellar bodies that are exported [49, 50]. Therefore, there is an important recycling function in addition to a degradation function in these cells. This could mean that more of the late endosomes are converted to recycling endosomes rather than fusing with lysosomes in the A549 cells.

Fig. 5 shows contrast enhanced images of C2C12 and A549 cells each labelled with antibodies against Rab5-561 (red), Rab7-633 (blue), and LAMP-1-488 (green).

It is evident from the appearance of yellow-orange regions and turquoise regions that there is some co-localization of these markers. Perfect co-localization of all three markers should lead to white regions, which are hard to observe in either image.

Table 6 summarizes the fractions of three-way co-localization as

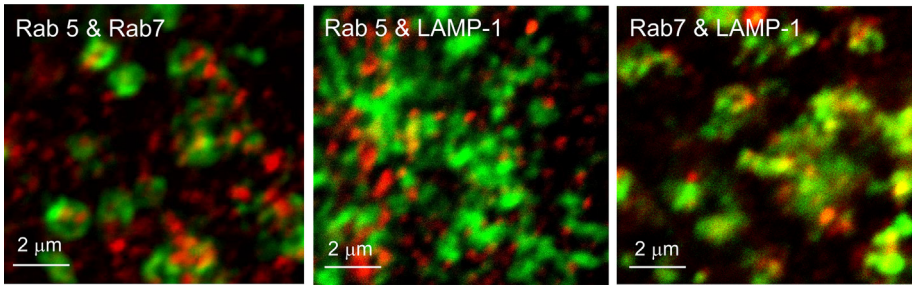

Fig. 4. Images of pairwise interaction of endocytic markers in C2C12 cells.

Table 4
Summary of fractions of co-localization in C2C12 cells.

$\langle F \rangle$	Rab5	Rab7	LAMP-1
Rab5	–	0.46 ± 0.05[1]	0.32 ± 0.05
Rab7	0.53 ± 0.06	–	0.74 ± 0.04
LAMP-1	0.31 ± 0.04	0.86 ± 0.03	–

[1] Standard error.

Table 5
Summary of fractions of co-localization in A549 cells.

$\langle F \rangle$	Rab5	Rab7	LAMP-1
Rab5	–	0.50 ± 0.03[1]	0.82 ± 0.04
Rab7	0.39 ± 0.03	–	0.26 ± 0.06
LAMP-1	0.80 ± 0.05	0.37 ± 0.06	–

[1] Standard error.

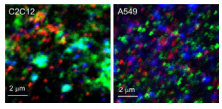

Fig. 5. Rab5, Rab7, and LAMP-1 marked endosomes in C2C12 & A549 cells.

Table 6
Extent of association of one marker with two markers of endosomes in C2C12 and A549 cells.

$\langle F(Marker \mid Two\ Markers) \rangle$	C2C12	A549
$\langle F(Rab5 \mid Rab7\ \ LAMP-1) \rangle$	0.56 ± 0.06[1]	0.16 ± 0.05
$\langle F(Rab7 \mid Rab5\ \ LAMP-1) \rangle$	0.42 ± 0.06	0.11 ± 0.03
$\langle F(LAMP-1 \mid Rab5\ \ Rab7) \rangle$	0.28 ± 0.05	0.08 ± 0.03

[1] Standard error.

calculated from Eqs. (9), (10), and (11) using TRICCS.

These data show that the extent of three-way co-localization is much greater in C2C12 cells than in A549 cells. Among those endosomes containing Rab5, about 56% also contain both Rab7 and LAMP-1 in C2C12 cells compared to about 16% in A549 cells. Likewise, among those endosomes containing Rab7, about 42% also contain both Rab5 and LAMP-1 compared to about 11% in A549 cells. Finally, among those lysosomes that contain LAMP-1, about 18% also contain both Rab5 and Rab7 compared to about 8% in A549 cells. It should be noted that the extent of three-way co-localization observed in the A549 cells is close to the limit of reliable detection and there may not be much, if any, co-localization when the number is less than about 10%. Nevertheless, these experiments confirm that in C2C12 cells there is a significant number of endosomes or lysosomes that contain all three markers, while in A549 cells there are only a few that may contain all three markers. This is consistent with the notion that in A549 cells many of the late endosomes are diverted to recycling endosomes rather than lysosomes and that the early lysosomes can fuse directly with the lysosomes.

6. Discussion

The quantitative analysis of the distribution and extent of clustering of the antibodies against the intracellular proteins Rab5, Rab7, and LAMP-1 reveal that they are highly clustered (on the order of 500–1000 antibodies per cluster), that these clusters are large (0.2–0.6 μm), and that they are distributed evenly intracellularly. These observations are consistent with each of these proteins being associated with organelles such as the endosomes and the lysosomes [51, 52, 53].

It is clear from the data presented here that the markers purported to represent early endosomes (Rab5), late endosomes (Rab7) and lysosomes (LAMP-1) are not as specific as previously reported with at least 30% and up to 80% co-localization of some of these markers on the same endosomes or lysosomes. This is not surprising if the maturation model is correct, since it is reasonable to expect that during a maturation process where Rab5 proteins are being cleared and Rab7 proteins are emerging, there will be a period when both proteins can co-exist in the same endosomes [54]. Likewise, if there is fusion of late endosomes with lysosomes, there may well be a period before the Rab7 proteins are fully cleared from the lysosomes after the fusion event. Out findings are therefore consistent with a maturation-fusion process.

With live cell imaging, Rink et al and Poteryaev et al. both successfully showed that Rab5 is replaced with Rab7 during endocytosis [26, 27]. In both works, images of cells were co-expressed with Rab5 and Rab7 fluorescent proteins and were imaged over time. In both studies, an increase of Rab7 fluorescent signal with a simultaneous decrease of Rab5 fluorescent signal was observed. Thus, these findings suggest a substitution of Rab5 by Rab7, but also *show* evidence for a point in time in which there is some degree of co-localization of the two markers on some endosomes. The work presented in this manuscript supports the notion that Rab5 is replaced with Rab7, and has quantified the extent of the coexistence of the two proteins. Our findings suggest that these markers are not as *unique* to a single compartment as commonly thought.

The observation that a significant amount of Rab5 is co-localized with LAMP-1 suggests that the maturation and fusion processes are less linear than the model might imply. In other words, it is possible that fusion of endosomes with lysosomes can occur well before the maturation process from early to late endosomes is complete. This is even more pronounced in the A549 cells, where there appears to be more lysosomes that contain Rab5 than contain Rab7, suggesting that the fusion process can precede the maturation process in these cells and supporting the notion that the late endosomes are targeted more to become recycling endosomes.

That the complete maturation from early to late endosomes is not a prerequisite for fusion is further supported by the evidence that all three proteins can co-exist to a significant extent, at least in the C2C12 cells. The smaller extent of three-way co-localization in A459 cells coupled with the higher degree of co-localization of Rab5 and LAMP-1 than Rab7 and LAMP-1 may indicate that there is a higher probability for early endosomes to fuse with lysosomes in these cells. Whether this is related to their function as cells that recycle liposome materials in the lung remains to be investigated [55, 56].

The application of triple cross correlation spectroscopy allowed us to

study the extent of Rab5, Rab7, and LAMP-1 in three-way fashion, which to the best of our knowledge has not previously been attempted. As a result, we learned Rab5, Rab7, and LAMP-1 can co-exist in the same intracellular organelles and that the extent to which they associate can vary significantly between different cell types.

Since the three proteins (Rab5, Rab7, and LAMP-1) can co-exist in the same intracellular organelles, it may be prudent to reevaluate their use as specific markers for specific endosomal or lysosomal entities. Moreover, if completion of the maturation process from early to late endosomes is not required for their fusion with the lysosomes, the linearity of the maturation-fusion model is in question.

We note that in this study we are not directly studying the dynamics of the endocytosis process but rather focus on the steady state distribution of the classical markers for components of the endocytosis pathway. Our conclusions are therefore limited to an understanding of their distribution in normally growing cells that have been fixed at an arbitrary point of time in the cell cycle.

Declarations

Author contribution statement

Lindsay Shearer: Conceived and designed the experiments; Performed the experiments; Analyzed and interpreted the data; Contributed reagents, materials, analysis tools or data; Wrote the paper.

Nils Petersen: Conceived and designed the experiments; Analyzed and interpreted the data; Wrote the paper.

Funding statement

This work was supported by a discovery grant from the Natural Sciences and Engineering Research Council of Canada to NOP.

Competing interest statement

The authors declare no conflict of interest.

Additional information

Supplementary content related to this article has been published online at https://doi.org/10.1016/j.heliyon.2019.e02375.

Acknowledgements

We would like to thank Dr. Xuejun Sun and Geraldine Baron from the Department of Experimental Oncology in the Cross Cancer Institute for assistance with image correlation spectroscopy. We would like to thank Angela Brigley and Cathy DeGuzman from the National Institute for Nanotechnology for providing use of facilities for immunofluorescence. For analysis with this image correlation spectroscopy software, images were converted with the help from Dr. Nick Smisdom, from.lsm to.bmp.

References

[1] M. Kaksonen, A. Roux, Mechanisms of clathrin-mediated endocytosis, Nat. Rev. Mol. Cell Biol. 19 (2018) 313–326.
[2] C.T. Ng, et al., Clathrin-mediated endocytosis of gold nanoparticles in vitro, Anat. Rec. 298 (2015) 418–427.
[3] H.-J. Lee, et al., Assembly-dependent endocytosis and clearance of extracellular alpha-synuclein, Int. J. Biochem. Cell Biol. 40 (2008) 1835–1849.
[4] B.D. Chithrani, A.A. Ghazani, W.C.W. Chan, Determining the size and shape dependence of gold nanoparticle uptake into mammalian cells, Nano Lett. 6 (2006) 662–668.
[5] H. Hillaireau, P. Couvreur, Nanocarriers' entry into the cell: relevance to drug delivery, Cell. Mol. Life Sci. 66 (2009) 2873–2896.
[6] M. Mettlen, P.-H. Chen, S. Srinivasan, G. Danuser, S.L. Schmid, Regulation of clathrin-mediated endocytosis, Annu. Rev. Biochem. 87 (2018) 871–896.
[7] D. Dutta, J.G. Donaldson, Rab and Arf G proteins in endosomal trafficking, Methods Cell Biol. 130 (2015) 127–138.
[8] A. Gautreau, K. Oguievetskaia, C. Ungermann, Function and regulation of the endosomal fusion and fission machineries, Cold Spring Harb. Perspect. Biol. 6 (2014).
[9] Endosomes, Landes Bioscience/Eurekah.Com, Springer Science+Business Media, 2006.
[10] A. Helenius, I. Mellman, D. Wall, A. Hubbard, Endosomes, Trends Biochem. Sci. 8 (1983) 245–250.
[11] J. Huotari, A. Helenius, Endosome maturation, EMBO J. 30 (2011) 3481–3500.
[12] P.R. Pryor, J.P. Luzio, Delivery of endocytosed membrane proteins to the lysosome, Biochim. Biophys. Acta Mol. Cell Res. 1793 (2009) 615–624.
[13] C. Le Roy, J.L. Wrana, Clathrin- and non-clathrin-mediated endocytic regulation of cell signalling, Nat. Rev. Mol. Cell Biol. 6 (2005) 112–126.
[14] H. Liewen, et al., Characterization of the human GARP (Golgi associated retrograde protein) complex, Exp. Cell Res. 306 (2005) 24–34.
[15] M. Podinovskaia, A. Spang, The endosomal network: mediators and regulators of endosome maturation, in: C. Lamaze, I. Prior (Eds.), Endocytosis and Signaling, Springer International Publishing, 2018, pp. 1–38.
[16] S.R. Pfeffer, Rab GTPase regulation of membrane identity, Curr. Opin. Cell Biol. 25 (2013) 414–419.
[17] H. Stenmark, V.M. Olkkonen, The Rab GTPase family, Genome Biol. 2 (2001) reviews3007.1.
[18] J.P. Gorvel, P. Chavrier, M. Zerial, J. Gruenberg, rab5 controls early endosome fusion in vitro, Cell 64 (1991) 915–925.
[19] A.H. Hutagalung, P.J. Novick, Role of Rab GTPases in membrane traffic and cell physiology, Physiol. Rev. 91 (2011) 119–149.
[20] C. Bucci, et al., The small GTPase rab5 functions as a regulatory factor in the early endocytic pathway, Cell 70 (1992) 715–728.
[21] M.A. Barbieri, et al., Evidence for a symmetrical requirement for rab5-GTP in in vitro endosome-endosome fusion, J. Biol. Chem. 273 (1998) 25850–25855.
[22] E. Nielsen, F. Severin, J.M. Backer, A.A. Hyman, M. Zerial, Rab5 regulates motility of early endosomes on microtubules, Nat. Cell Biol. 1 (1999) 376–382.
[23] L. Goto-Silva, et al., Retrograde transport of Akt by a neuronal Rab5-APPL1 endosome, Sci. Rep. 9 (2019) 1–14.
[24] N. Epp, R. Rethmeier, L. Krämer, C. Ungermann, Membrane dynamics and fusion at late endosomes and vacuoles–Rab regulation, multisubunit tethering complexes and SNAREs, Eur. J. Cell Biol. 90 (2011) 779–785.
[25] T. Wang, Z. Ming, W. Xiaochun, W. Hong, Rab7: role of its protein interaction cascades in endo-lysosomal traffic, Cell. Signal. 23 (2011) 516–521.
[26] J. Rink, E. Ghigo, Y. Kalaidzidis, M. Zerial, Rab conversion as a mechanism of progression from early to late endosomes, Cell 122 (2005) 735–749.
[27] D. Poteryaev, S. Datta, K. Ackema, M. Zerial, A. Spang, Identification of the switch in early-to-late endosome transition, Cell 141 (2010) 497–508.
[28] J.-M. Cioni, et al., Late endosomes act as mRNA translation platforms and sustain mitochondria in axons, Cell 176 (2019) 56–72, e15.
[29] C. Bucci, P. Thomsen, P. Nicoziani, J. McCarthy, B. van Deurs, Rab7: a key to lysosome biogenesis, Mol. Biol. Cell 11 (2000) 467–480.
[30] S. Jäger, et al., Role for Rab7 in maturation of late autophagic vacuoles, J. Cell Sci. 117 (2004) 4837–4848.
[31] E.-L. Eskelinen, Roles of LAMP-1 and LAMP-2 in lysosome biogenesis and autophagy, Mol. Asp. Med. 27 (2006) 495–502.
[32] S. Kornfeld, I. Mellman, The biogenesis of lysosomes, Annu. Rev. Cell Biol. 5 (1989) 483–525.
[33] L. Wartosch, N.A. Bright, J.P. Luzio, Lysosomes, Curr. Biol. 25 (2015) R315–R316.
[34] A. Ikari, et al., Clathrin-dependent endocytosis of claudin-2 by DFYSP peptide causes lysosomal damage in lung adenocarcinoma A549 cells, Biochim. Biophys. Acta 1848 (2015) 2326–2336.
[35] M. Studzian, G. Bartosz, L. Pulaski, Endocytosis of ABCG2 drug transporter caused by binding of 5D3 antibody: trafficking mechanisms and intracellular fate, Biochim. Biophys. Acta 1853 (2015) 1759–1771.
[36] B. Kasmapour, L. Cai, M.G. Gutierrez, Spatial distribution of phagolysosomes is independent of the regulation of lysosome position by Rab34, Int. J. Biochem. Cell Biol. 45 (2013) 2057–2065.
[37] J.Z. Rappoport, S.M. Simon, Endocytic trafficking of activated EGFR is AP-2 dependent and occurs through preformed clathrin spots, J. Cell Sci. 122 (2009) 1301–1305.
[38] N. Jouvenet, M. Zhadina, P.D. Bieniasz, S.M. Simon, Dynamics of ESCRT protein recruitment during retroviral assembly, Nat. Cell Biol. 13 (2011) 394–401.
[39] J.Z. Rappoport, S. Kemal, A. Benmerah, S.M. Simon, Dynamics of clathrin and adaptor proteins during endocytosis, Am. J. Physiol. Cell Physiol. 291 (2006) C1072–1081.
[40] J.Z. Rappoport, K.P. Heyman, S. Kemal, S.M. Simon, Dynamics of dynamin during clathrin mediated endocytosis in PC12 cells, PLoS One 3 (2008) e2416.
[41] A. Yoshida, et al., Morphological changes of plasma membrane and protein assembly during clathrin-mediated endocytosis, PLoS Biol. 16 (2018) e2004786.
[42] N.O. Petersen, et al., Analysis of membrane protein cluster densities and sizes in situ by image correlation spectroscopy, Faraday Discuss (1998) 289–305, discussion 331-343.
[43] D.L. Kolin, P.W. Wiseman, Advances in image correlation spectroscopy: measuring number densities, aggregation states, and dynamics of fluorescently labeled macromolecules in cells, Cell Biochem. Biophys. 49 (2007) 141–164.
[44] M. Wang, N.O. Petersen, Lipid-coated gold nanoparticles promote lamellar body formation in A549 cells, Biochim. Biophys. Acta 1831 (2013) 1089–1097.
[45] W. Zhang, et al., Influence of cell physiological state on gene delivery to T lymphocytes by chimeric adenovirus Ad5F35, Sci. Rep. 6 (2016) 22688.
[46] L.M.P. Vermeulen, et al., Endosomal size and membrane leakiness influence proton sponge-based rupture of endosomal vesicles, ACS Nano 12 (2018) 2332–2345.

[47] J.R. Abney, B.A. Scalettar, C.R. Hackenbrock, On the measurement of particle number and mobility in nonideal solutions by fluorescence correlation spectroscopy, Biophys. J. 58 (1990) 261–265.
[48] P.R. St-Pierre, N.O. Petersen, Average density and size of microclusters of epidermal growth factor receptors on A431 cells, Biochemistry 31 (1992) 2459–2463.
[49] K.A. Foster, C.G. Oster, M.M. Mayer, M.L. Avery, K.L. Audus, Characterization of the A549 cell line as a type II pulmonary epithelial cell model for drug metabolism, Exp. Cell Res. 243 (1998) 359–366.
[50] S.-H. Yu, F. Possmayer, Lipid compositional analysis of pulmonary surfactant monolayers and monolayer-associated reservoirs, J. Lipid Res. 44 (2003) 621–629.
[51] X.-T. Cheng, et al., Characterization of LAMP1-labeled nondegradative lysosomal and endocytic compartments in neurons, J. Cell Biol. 217 (2018) 3127–3139.
[52] C. Stroupe, This is the end: regulation of Rab7 nucleotide binding in endolysosomal trafficking and autophagy, Front. Cell Dev. Biol. 6 (2018).
[53] H. Shimamura, M. Nagano, K. Nakajima, J.Y. Toshima, J. Toshima, Rab5-independent activation and function of yeast Rab7-like protein, Ypt7p, in the AP-3 pathway, PLoS One 14 (2019) e0210223.
[54] F.R. Kiral, F.E. Kohrs, E.J. Jin, P.R. Hiesinger, Rab GTPases and membrane trafficking in neurodegeneration, Curr. Biol. 28 (2018) R471–R486.
[55] J.U. Balis, S.D. Bumgarner, J.E. Paciga, J.F. Paterson, S.A. Shelley, Synthesis of lung surfactant-associated glycoproteins by A549 cells: description of an in vitro model for human type II cell dysfunction, Exp. Lung Res. 6 (1984) 197–213.
[56] D.L. Shapiro, L.L. Nardone, S.A. Rooney, E.K. Motoyama, J.L. Munoz, Phospholipid biosynthesis and secretion by a cell line (A549) which resembles type II alveolar epithelial cells, Biochim. Biophys. Acta Lipids Lipid Metab. 530 (1978) 197–207.